Chinese Chemical Letters 31 (2020) 1382–1386

Contents lists available at ScienceDirect

Chinese Chemical Letters

journal homepage: www.elsevier.com/locate/cclet

Communication

Tumor-homing peptide-based NIR-II probes for targeted spontaneous breast tumor imaging

Hui Zhou[a,b,1], Shanshan Li[b,1], Xiaodong Zeng[b], Mengxian Zhang[b], Lin Tang[b], Qianqian Li[b], Deliang Chen[d,*], Xianli Meng[a,**], Xuechuan Hong[a,b,c,**]

[a] Innovative Institute of Chinese Medicine and Pharmacy, Chengdu University of Traditional Chinese Medicine, Chengdu 611137, China
[b] Key Laboratory of Combinatorial Biosynthesis and Drug Discovery (MOE), Hubei Province Engineering and Technology Research Center for Fluorinated Pharmaceuticals, Shenzhen Institute of Wuhan University, Shenzhen 518057, China
[c] College of Science, Innovation Center for Traditional Tibetan Medicine Modernization and Quality Control, Medical College, Tibet University, Lasa 850000, China
[d] Jiangxi Key Laboratory of Organo-Pharmaceutical Chemistry, Chemistry and Chemical Engineering College, Gannan Normal University, Ganzhou 341000, China

ARTICLE INFO

Article history:
Received 4 March 2020
Received in revised form 8 April 2020
Accepted 16 April 2020
Available online 19 April 2020

Keywords:
NIR-II imaging
F3 peptide
Image-guided surgery
Spontaneous breast carcinoma
NIR-II probes

ABSTRACT

Fluorescence imaging in the second near-infrared window (NIR-II, 1000–1700 nm) is a promising modality for real-time imaging of cancer and image-guided surgery with superior *in vivo* optical properties. So far, very few NIR-II fluorophores have been reported for *in vivo* biomedical imaging of chemically-induced spontaneous breast carcinoma. Herein, a NIR-II fluorescent probe **CH1055-F3** with the nucleolin-targeted tumor-homing peptide **F3** was demonstrated to preferentially accumulate in 4T1 tumors. More importantly, **CH1055-F3** exhibited specific NIR-II signals with high spatial and temporal resolution, strong tumor uptake, and remarkable NIR-II image-guided surgery in dimethylbenzanthracene (DMBA)-induced spontaneous breast tumor rats. This report presents the first tumor-homing peptide-based NIR-II probe to diagnose transplantable and spontaneous breast tumors by the active targeting.

Breast cancer is one of the most common malignant cancers among women in the world, which affects countries at all levels of modernization [1–3]. It accounts for ~30% of new cases and is the second leading cause of cancer deaths in females [4]. Medical imaging such as computed tomography (CT), magnetic resonance imaging (MRI) or positron emission tomography (PET) has intensively used in all phases of breast cancer detection, therapy monitoring and post-therapeutic follow-up. However, current clinical imaging techniques have some limitations for studying *in vivo* biological changes in relation with diagnosis, carcinogenesis, therapy response and prognosis [5]. *In vivo* fluorescence imaging in the first near-infrared window (700–900 nm, NIR-I), such as indocyanine green (ICG), has been widely used for early diagnosis and image-guided sentinel lymph node biopsy of breast cancer in clinic over the last decade [6–10]. Recently, NIR-II fluorescence imaging (1000–1700 nm) has achieved a higher tumor-to-normal tissue ratio, excellent temporal and spatial resolutions, deeper imaging depths, and opened up a new era for small molecular imaging [11,12]. Particularly, NIR-IIb sub-window (1500–1700 nm) shows tremendous benefits of negligible scattering, near-zero auto-fluorescence, and unparalleled tissue-imaging depths on *in vivo* fluorescence bioimaging [13–16]. So far, numerous inorganic and organic NIR-II, NIR-IIa (1300–1400 nm) and NIR-IIb probes, such as quantum dots (QDs) [17–21], single-walled carbon nanotubes (SWNTs) [22,23], ultra-small gold clusters [24,25], rare-earth down-conversion nanoparticles (DCNPs) [26–28], and small organic dyes [29–44] have been discovered. It is worth noting that a novel small organic molecule **H3-PEG2K** exhibits excellent passive targeting ability and precise delineation of chemically-induced spontaneous breast cancer [45]. However, small-molecule NIR-II fluorophores are still in its fancy, and NIR-II fluorescence imaging of spontaneous breast tumors by the active targeting has not been reported yet.

Nucleolin, a receptor protein, traffics between membrane, cytoplasm, and nucleus [46]. Nucleolin is usually over-expressed

* Corresponding author.
** Corresponding authors at: Key Laboratory of Combinatorial Biosynthesis and Drug Discovery (MOE), Hubei Province Engineering and Technology Research Center for Fluorinated Pharmaceuticals, Shenzhen Institute of Wuhan University, Shenzhen 518057, China.
E-mail addresses: dechen@gnnu.cn (D. Chen), xlm999@cdutcm.edu.cn (X. Meng), xhy78@whu.edu.cn (X. Hong).
[1] These two authors contributed equally to this work.

https://doi.org/10.1016/j.cclet.2020.04.030
1001-8417/

on the membrane of breast cancer cells [47], indicating the potential of nucleolin to be a biomarker for breast cancer targeted imaging and therapy. The tumor-homing peptide **F3**, an N terminal fragment of human high mobility group protein 2 (HMGN2, formerly HMG-17) with 31-amino acid sequence (KDEPQRRSARLSAKPAPPKPEPKPKKAPAKK), was first obtained from screening phage of mice bone marrow cells *in vitro* and from homing to HL-60 human leukemia tumor xenografts *in vivo* [48,49]. **F3** selectively targets cell-surface nucleolin in breast tumor cells and tumor endothelial cells. It also exhibits cell-penetrating properties with high cellular uptake in previous research. Therefore, it is desirable to designthe highlytumor-specific NIR-IIimaging probes based on **F3** peptide.

Herein, we have rationally designed and synthesized a tumor-homing peptide-based NIR-II probe **CH1055-F3** for targeted subcutaneous 4T1 xenografts and spontaneous breast tumor imaging. **CH1055-F3** exhibited excellent specificity to 4T1 breast cancer and spontaneous breast cancer induced by the chemical reagent dimethylbenzanthracene (DMBA) [50]. To the best of our knowledge, it is the first time to develop a NIR-II probe to image both transplantable and spontaneous breast cancer through active targeting in the NIR-II window. Besides, image-guided tumor resection surgery for spontaneous breast tumor bearing rats was carried out in the NIR-II window, providing a promising method for tumor excision in clinic.

The tumor-homing peptide **F3** has demonstrated a high specificity and affinity to nucleolin in breast tumor cells. **F3** peptide was modified by an extra cysteine amino acid (Cys) in order to improve the reaction yield througha facile maleimide-thiol coupling reaction with a NIR-II dye **CH1055-Mal**. The NIR-II fluorophore **CH1055** with four carboxyl groups was first amidated with maleimide to afford **CH1055-Mal**. Afterwards, the targeting peptide **F3**-Cys was conjugated to the intermediate **CH1055-Mal** based on a maleimide-thiol coupling reaction to obtain the mono-substituted **CH1055-F3** in 49% yield (Scheme 1). The structure was confirmed by MALDI-TOF-MS. The UV–vis-NIR absorption and fluorescence spectra of **CH1055-F3** in water (Fig. 1A) indicated that the maximum absorption peak was ~726 nm and the maximum emission peak was ~1020 nm with the large stokes shift of 294 nm. Meanwhile, **CH1055-F3** exhibited excellent photostability in PBS for 60 min (Fig. 1B).

The 4T1 cell lines and HepG2 cell lines were applied to evaluate the potential cytotoxicity of **CH1055-F3** by a standard 3-(4,5-dimethylthiazol-2-yl)-2,5-diphenyl tetrazolium bromide (MTT) assay. As shown in Fig. 2A and Fig. S2 (Supporting information), no obvious toxicity was observed in both 4T1 and HepG2 cells and ~100 % viability was shown at various dosages, suggesting the excellent biocompatibility of **CH1055-F3** and great potential for *in vivo* bioimaging. **CH1055-F3** was then injected into KM mice (5 μg/g) through the tail vein. The results demonstrated that **CH1055-F3** was mainly distributed in the liver and kidneys (Fig. 2C). *Ex vivo* distribution results illustrated that the clearance route of this imaging agent was mainly *via* the hepatobiliary and renal systems. Through the quantitative analysis of major organs (Fig. 2D), the fluorescent signals of liver and kidneys were significantly higher than those of other organs (heart, lung and spleen). Meanwhile, the blood samples were collected from 0 to 10 h to measure the fluorescent intensity, and the half-life of

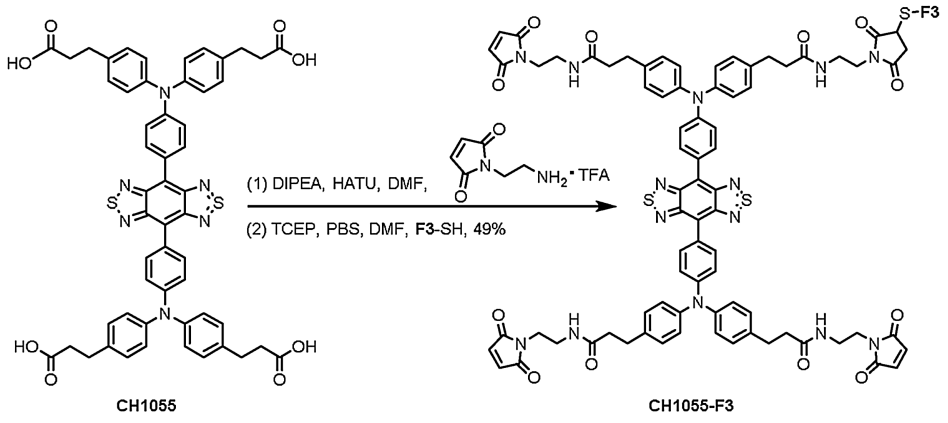

F3-SH: Lys-Asp-Glu-Pro-Gln-Arg-Arg-Ser-Ala-Arg-Leu-Ser-Ala-Lys-Pro-Ala-Pro-Pro-Lys-Pro-Glu-Pro-Lys-Pro-Lys-Lys-Ala-Pro-Ala-Lys-Lys-Cys

Scheme 1. The synthetic route of **CH1055-F3**.

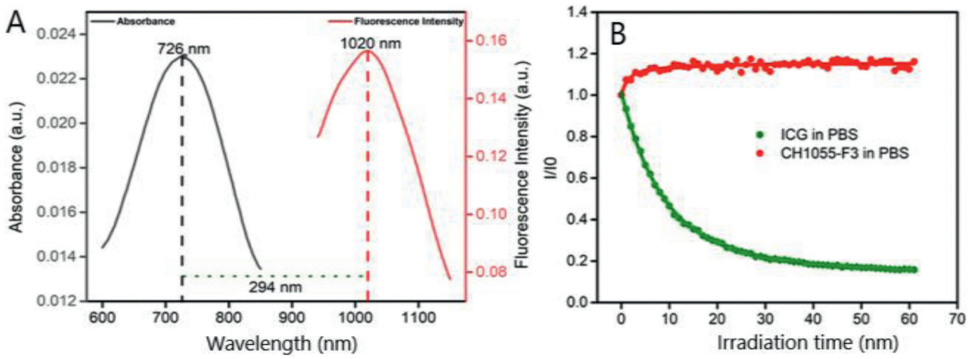

Fig. 1. (A) The absorption and emission spectra of **CH1055-F3**. (B) The photostability of **CH1055-F3** and ICG in PBS solutions under continuous 808 nm laser irradiation.

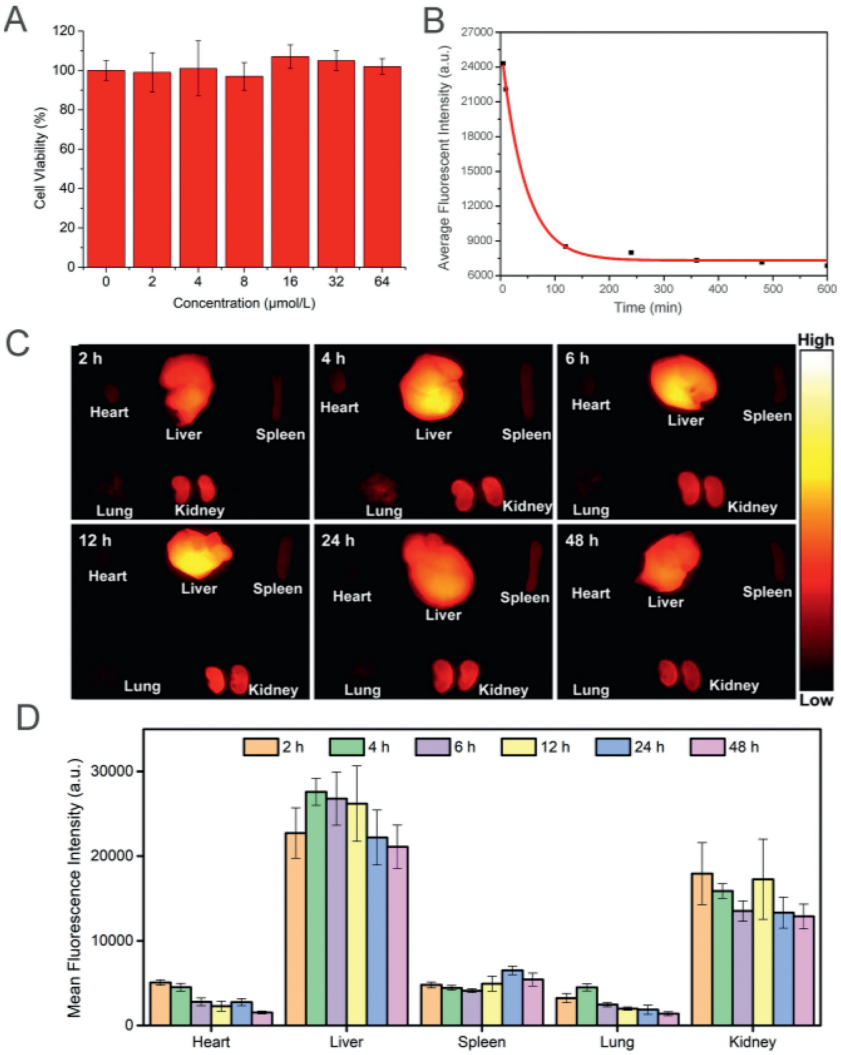

Fig. 2. (A) Cell viability of 4T1 breast cancer cells incubated with **CH1055-F3** at different concentrations. (B) Blood circulation half-life curve of **CH1055-F3** in mice using a first-order exponential decay ($n = 3$). (C) *Ex vivo* NIR-II fluorescent images of major organs in KM mice treated with **CH1055-F3** ($n = 3$). (D) Quantitative analysis of fluorescent intensity of the major organs in (C) at various time points.

CH1055-F3 in blood was calculated to be ~43.3 min based on the equation $y = 7310.91 + 18878.66e^{-x/43.11}$) as shown in Fig. 2B, exhibiting the rapid whole-body elimination.

In vivo targeting experiments were first carried out in the subcutaneous 4T1 cells of tumor-bearing Balb/c mice. The mice ($n = 3$) were intravenously (i.v.) injected with 200 μL of PBS solution containing 0.2 mg **CH1055-F3** through the tail vein when the tumor volumes reached at 400 ~ 800 mm^3. The non-invasive NIR-II fluorescence imaging was performed on an InGaAs camera. As shown in Fig. 3, the 4T1 tumor was easily differentiated from the surrounding normal tissues. The intensity of fluorescence was increased from 2 h to 24 h, and reached the maximum at 10 h with a tumor signals/normal tissue signals (T/NT) value of 4.9 (Fig. 3 and Fig. S3 in Supporting information).

The transplanted, genetically engineered or environmentally caused such as chemically induced animal cancer models have been used to mimic different human cancer pathologies and address various research questions. The chemically induced spontaneous primary cancer models can simulate the originality, evolution and consequence of clinical cancer process, and are ideally used to investigate the etiology, prevention, diagnosis and treatment of cancer. Accordingly, a spontaneous DMBA-induced carcinoma model using Sprague Dawley (SD) female rats, comparable to the actual human breast tumors, was established to investigate the feasibility of **CH1055-F3** for the tumor-homing targeted NIR-II imaging and image-guided surgery. SD rats were orally fed DMBA suspension in soya bean oil (20 mg/mL) at a dosage of 200 mg/kg in 10–15 weeks until the diameter of the primary tumors reached 10–20 mm. Subsequently, **CH1055-F3** (2 mg in 1 mL PBS) was administrated into a DMBA-induced mammary carcinoma rat ($n = 3$) by intravenous injection and NIR-II fluorescence images of rat tumors were obtained at various time points (Fig. 4A). Three tumors on the SD rats were significantly visualized and delineated from the surrounding background tissues with the assistance of NIR-II imaging at 48 h. As shown in Fig. 4B, the process of the tumor resection was demonstrated, three tumors were successfully dissected and removed from the surrounding normal tissue. Specimen **1** with strong fluorescent NIR-II signals was stained with hematoxylin and eosin assessed (Figs. S5B and C in Supporting information). Histological analysis of specimen **1** has shown that the histological characteristics of normal tissues were almost not detected.

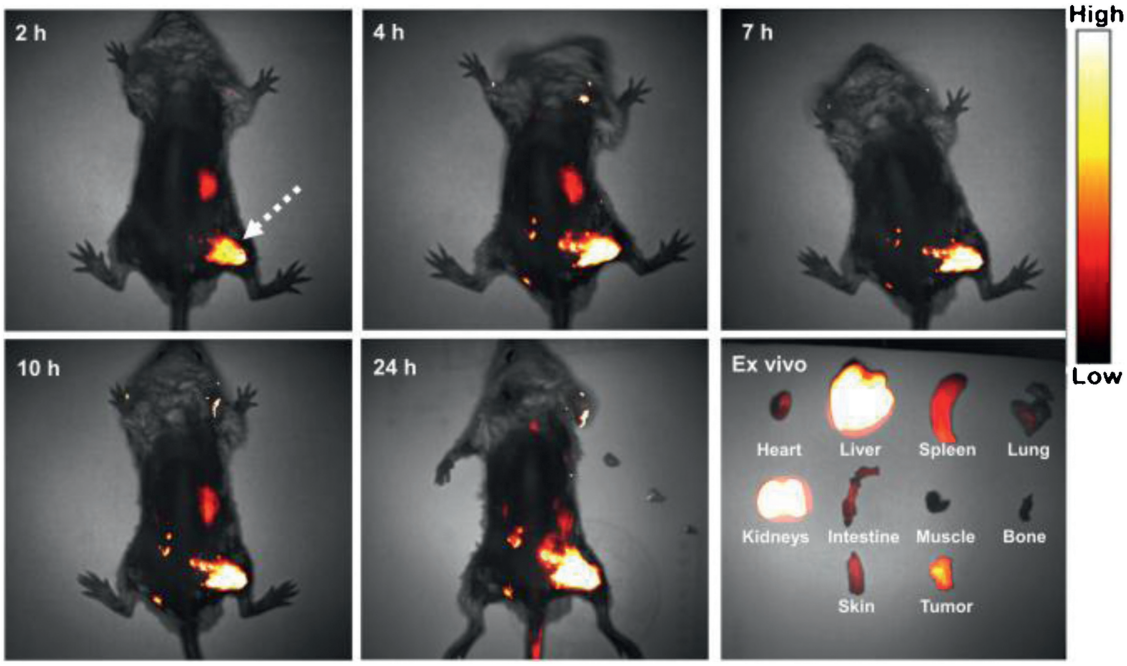

Fig. 3. The representative photograph and *in vivo* NIR-II fluorescence images of Balb/c mice bearing 4T1 tumorat 2, 4, 7, 10 and 24 h after intravenous injection. All the NIR-II images were obtained from an InGaAs camera with 50 ms exposure time using 1000 nm long-pass filter under an 808 nm laser excitation at a power density of 90 mW/cm^2. The white arrow indicates the location of 4T1 tumor in the right leg of mice.

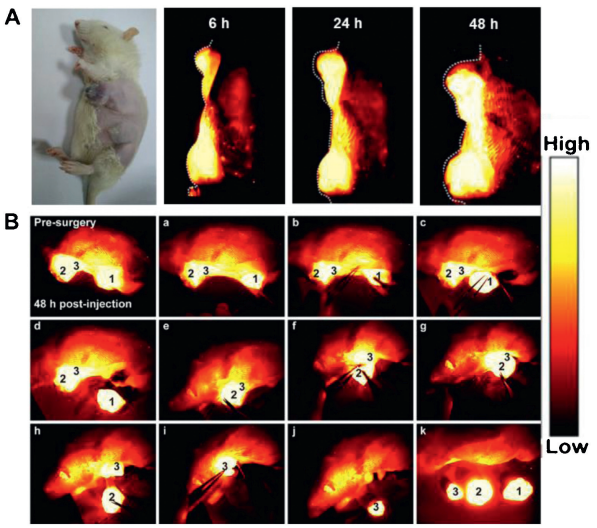

Fig. 4. (A) The representative NIR-II fluorescence images (1000 nm LP, 300 ms exposure, 90 mW/cm^2, 808 nm laser irradiation) of a SD rat with DMBA-induced mammary carcinoma 6 h, 24 h and 48 h after i.v. injection of 1 mL **CH1055-F3** (2 mg per rat) PBS solution. (B) NIR-II image-guided surgery 48 h after i.v. injection of the probe into a SDrat with DMBA-induced mammary carcinoma operated in 250 ms exposure and 1000 nm long-pass filter under 808 nm laser excitation with a power density of 90 mW/cm^2.

In summary, a NIR-II probe **CH1055-F3** for tumor-specific imaging and imaging-guided surgery was successfully constructed *via* amidation and click reactions based on the dye **CH1055** and **F3** peptide. **CH1055-F3** possessed excellent photo-stability, biocompatibility and tumor-specific ability, which showed excellent nucleolin-targeting performance in both transplantable and spontaneous breast cancer. Besides, image-guide surgery was successfully performed on the chemically DMBA-induced breast cancer rats. To the best of our knowledge, this is the first time that nucleolin-targeted NIR-II imaging for non-invasive tumor diagnosis of chemically induced spontaneous breast cancer and image-guided surgery in DMBA-induced mammary carcinoma rat was reported other than the xenograft model. This work provides a new approach to develop NIR-II probes to diagnose and excise tumor in clinic research. Moreover, this conception to design the NIR-II probes could enrich the filed for *in vivo* bioimaging, tumor targeting and various therapeutic applications in the future.

Declaration of competing interest

The authors declare no conflict of interest.

Acknowledgments

This work was partially supported by grants from the National Natural Science Foundation of China (Nos. 81773674, 21473041 and 81573383), Project First-Class Disciplines Development Supported by Chengdu University of Traditional Chinese Medicine (No. CZYJC1903), Natural Science Foundation of Hubei Province (Nos. 2017CFA024, 2016ACA126 and 2017CFB711), the Applied Basic Research Program of Wuhan Municipal Bureau of Science and Technology (No. 2019020701011429), Shenzhen Science and Technology Research Grant (No. JCYJ20190808152019182), Tibet Autonomous Region Science and Technology Plan Project Key Project (No. XZ201901-GB-11), the Fundamental Research Funds for the Central Universities, and Health Commission of Hubei Province Scientific Research Project (Nos. WJ2019M177 and WJ2019M178).

Appendix A. Supplementary data

Supplementary material related to this article can be found, in the online version, at doi:https://doi.org/10.1016/j.cclet.2020.04.030.

References

[1] H. Guo, J. Lu, H. Hathaway, et al., Bioconjugate Chem. 22 (2011) 1682–1689.
[2] O. Ginsburg, F. Bray, M.P. Coleman, et al., Lancet 389 (2017) 847–860.

[3] C.E. DeSantis, S.A. Fedewa, A. Goding Sauer, et al., CA-Cancer J. Clin. 66 (2016) 31–42.
[4] R. Bam, M. Laffey, K. Nottberg, et al., Bioconjugate Chem. 30 (2019) 1677–1689.
[5] C. Tang, Y. Du, Q. Liang, et al., Mol. Pharmaceut. 15 (2018) 4702–4709.
[6] C. Yan, L. Shi, Z. Guo, et al., Chin. Chem. Lett. 30 (2019) 1849–1855.
[7] X. Luo, J. Li, J. Zhao, et al., Chin. Chem. Lett. 30 (2019) 839–846.
[8] Y. Zhang, H. Teng, Y. Gao, et al., Chin. Chem. Lett. (2020), doi:http://dx.doi.org/10.1016/j.cclet.2020.03.020.
[9] D. Shi, S. Chen, B. Dong, et al., Chem. Sci. 10 (2019) 3715–3722.
[10] L. Li, Y. Chen, W. Chen, et al., Chin. Chem. Lett. 30 (2019) 1689–1703.
[11] C. Li, Q. Wang, ACS Nano 12 (2018) 9654–9659.
[12] L. Tu, Y. Xu, Q. Ouyang, et al., Chin. Chem. Lett. 30 (2019) 1731–1737.
[13] C. Sun, B. Li, M. Zhao, et al., J. Am. Chem. Soc. 141 (2019) 19221–19225.
[14] Y. Li, Y. Liu, Q. Li, et al., Chem. Sci. 11 (2020) 2621–2626.
[15] Q. Li, Q. Ding, Y. Li, et al., Chem. Commun. 56 (2020) 3289–3292.
[16] Y. Li, Z. Cai, J. Qian, et al., Nat. Commun. 11 (2020) 1255.
[17] X. Hao, C. Li, Y. Zhang, et al., Adv. Mater. 30 (2018) 1804437.
[18] H. He, Y. Lin, Z. Tian, et al., Small 14 (2018) 1703296.
[19] C. Li, F. Li, Y. Zhang, et al., ACS Nano 9 (2015) 12255–12263.
[20] C. Li, Y. Zhang, M. Wang, et al., Biomaterials 35 (2014) 393–400.
[21] C. Zhu, G. Chen, Z. Tian, et al., Small 13 (2017) 1602309.
[22] G. Hong, J.C. Lee, J.T. Robinson, et al., Nat. Med. 18 (2012) 1841–1846.
[23] G. Hong, S. Diao, J. Chang, et al., Nat. Photonics 8 (2014) 723–730.
[24] H. Liu, G. Hong, Z. Luo, et al., Adv. Mater. 31 (2019) 1901015.
[25] Y. Chen, D.M. Montana, H. Wei, et al., Nano Lett. 17 (2017) 6330–6334.
[26] Y. Fan, P. Wang, Y. Lu, et al., Nat. Nanotechnol. 13 (2018) 941–946.
[27] P. Wang, Y. Fan, L. Lu, et al., Nat. Commun. 9 (2018) 2898.
[28] Y. Zhong, Z. Ma, S. Zhu, et al., Nat. Commun. 8 (2017) 737.
[29] B. Ding, Y. Xiao, H. Zhou, et al., J. Med. Chem. 62 (2019) 2049–2059.
[30] X. Zeng, Y. Xiao, J. Lin, et al., Adv. Healthcare Mater. 7 (2018) 1800589.
[31] Y. Sun, M. Ding, X. Zeng, et al., Chem. Sci. 8 (2017) 3489–3493.
[32] J. Lin, X. Zeng, Y. Xiao, et al., Chem. Sci. 10 (2019) 1219–1226.
[33] A.L. Antaris, H. Chen, K. Cheng, et al., Nat. Mater. 15 (2016) 235–242.
[34] B. Li, L. Lu, M. Zhao, et al., Angew. Chem. Int. Ed. 57 (2018) 7483–7487.
[35] J. Yang, Q. Xie, H. Zhou, et al., J. Proteome Res. 17 (2018) 2428–2439.
[36] H. Zhou, H. Yang, L. Tang, et al., J. Mater. Chem. C 7 (2019) 9448–9454.
[37] Y. Sun, C. Qu, H. Chen, et al., Chem. Sci. 7 (2016) 6203–6207.
[38] H. Zhou, W. Yi, A. Li, et al., Adv. Healthcare Mater. 9 (2019) 1901224.
[39] H. Zhou, Y. Xiao, X. Hong, Chin. Chem. Lett. 29 (2018) 1425–1428.
[40] A.L. Antaris, H. Chen, S. Diao, et al., Nat. Commun. 8 (2017) 15269.
[41] Y. Sun, X. Zeng, Y. Xiao, et al., Chem. Sci. 9 (2018) 2092–2097.
[42] C. Qu, Y. Xiao, H. Zhou, et al., Adv. Opt. Mater. 7 (2019) 1900229.
[43] J. Lin, Q. Li, X. Zeng, et al., Sci. China Chem. 63 (2020) 766–770.
[44] J. Yang, X. Hong, Sci. China Chem. 62 (2019) 7–8.
[45] X. Zeng, L. Xie, D. Chen, et al., Chem. Commun. 55 (2019) 14287–14290.
[46] X. Fu, C. Liang, F. Li, et al., Int. J. Mol. Sci. 19 (2018) 1445.
[47] B. Cornelissen, A. Waller, C. Target, et al., Ejnmmi Res. 2 (2012) 9.
[48] K. Porkka, P. Laakkonen, J.A. Hoffman, et al., Proc. Natl. Acad. Sci. U. S. A. 99 (2002) 7444–7449.
[49] Y. Zhang, M. Yang, J. Park, et al., Small 5 (2009) 1990–1996.
[50] Y. Liu, T. Yin, Y. Feng, et al., Quant. Imag. Med. Surg. 5 (2015) 708–729.